Int. J. Heat Mass Transfer. Vol. 19, pp. 313–321. Pergamon Press 1976. Printed in Great Britain

TWO-FLUX SPHERICAL HARMONIC MODELLING OF TWO-DIMENSIONAL RADIATIVE TRANSFER IN FURNACES

NEVIN SELÇUK* and R. G. SIDDALL
Department of Chemical Engineering and Fuel Technology,
University of Sheffield, Sheffield S1 3JD, England

(*Received* 6 *May* 1975)

Abstract—A new two-flux model for two-dimensional radiation fields in axisymmetrical furnaces has been derived from radiative transport equations based on the P_1 spherical harmonic approximation by assuming radial polynomial variation of some radiation parameters, and applying an averaging procedure. The new model has been applied to the prediction of the thermal behaviour of an idealised radiant cell of a multipass process gas heater, and the results have been compared with previous values obtained using the zone method of analysis, and with limited experimental data from an operating heater. Satisfactory predictions are obtained for gas and surface temperature distributions, and for the overall thermal behaviour of the cell. This predictive accuracy, coupled with their computational simplicity and economy compared with the zone method of analysis, suggests that two-flux models of this type should prove to be useful tools for approximate thermal design calculations for axi-symmetrical furnaces and combustors.

NOMENCLATURE

A_G, cross sectional area of furnace gas space;
B, constant related to b, r_p and ε_p;
c, mass specific heat of gas;
C, constant related to b, B and r_p;
D, overall thermal resistance;
E, black body emissive power;
f, fraction of fuel burnt at height z;
F, radiation view factor;
G, incident flux density of radiation at a point;
K_a, volumetric absorption coefficient of furnace gas;
L, height;
L_f, flame length;
$\dot{m}$, mass flow rate;
n, total number of passes in one batch of tubes;
N, number of batches of tubes;
q, flux density;
q^+, radiant flux density in increasing co-ordinate direction;
q^-, radiant flux density in decreasing co-ordinate direction;
Q, net calorific value of fuel;
r, distance measured from axis of symmetry;
S, one half of the total tube surface area per unit volume of furnace gas space;
T, absolute temperature;
T_b, absolute base temperature;
z, distance measured from base of enclosure.

Greek symbols

β, constant related to F_{pt}, F_{tp} and ε_t;
ε, emissivity;
θ, angular co-ordinate;
σ, Stefan–Boltzmann constant;
ϕ, term neglected in process gas energy balance;
ψ, constant.

Subscripts

ad, at adiabatic flame temperature;
F, fuel;
g, process gas;
G, furnace gas;
i, number of pass;
j, k, tube numbers;
ij, for sector between ith and jth tubes;
m, arithmetic mean value or angular mean value;
p, effective value for equivalent grey surface;
r, radial direction;
R, refractory;
t, tube surface;
z, axial direction;
ξ, co-ordinate direction ($\xi = r$ or z).

*Now at Middle East Technical University, Ankara, Turkey.

1. INTRODUCTION

THE DESIGN of industrial furnaces and combustors is usually based on extremely simple mathematical modelling of the flow, reaction and heat exchange within the enclosure, of which the single-gas-zone treatment originally proposed by Lobo and Evans [1], and subsequently modified by Hottel [2, 3], provides a typical example. Such simple modelling of the physical situation has the advantage that the derived equations describing the overall thermal performance are algebraic in form, and, therefore, the numerical calculations involved in the design of a particular enclosure are straightforward and economical. However, these models are not without disadvantages; their use requires considerable experience and know-how in order to be able to allocate realistic values to certain dimensionless constants which occur in the working equations, and they do not provide a knowledge of the distributions of temperature and heat flux at the sink and refractory surfaces, which is desirable if local peak

values which might lead to material failure are to be avoided.

In recent years considerable research effort has been devoted to the development of more realistic and detailed models of enclosure behaviour which account for multidimensional variations of properties within the enclosure [4, 5]. However, these procedures suffer from the disadvantages of being computationally complex, involving computing expertise and expense which are several orders of magnitude greater than those associated with the simple models. These computational problems, coupled with uncertainties in the turbulent exchange parameters on which the predictions are based, has meant that such models have not proved attractive enough to ensure their wide employment by industrial designers.

What are required for design purposes at the present time are mathematical models which lie between the two extremes described above in both computational complexity and immediate applicability, providing a value for overall thermal performance together with predictions of the magnitudes and locations of the peak surface temperatures and heat fluxes.

At the high temperatures encountered in most furnaces thermal radiation is the predominant mechanism of heat transfer. Any successful treatment of enclosure performance must, therefore, be based on a reasonably realistic model of the radiation field. One of the most accurate procedures available for the prediction of radiative behaviour is the zone method of analysis [6]. Its limitation lies in the excessive storage capacity required for its execution, even with relatively coarse zoning. This has led to the investigation and use of flux methods [7, 8] as simpler and more economical, albeit less accurate, alternatives for the theoretical prediction of radiation. Conventional flux methods are based on the assumption that the intensity of radiation at a point is uniform but different within each of several smaller solid angles into which the total solid angle surrounding the point is subdivided, with discontinuous changes in intensity with direction occurring at the junction of any two adjacent smaller solid angles. Such physically unrealistic discontinuities can, however, be avoided by representing the angular distribution of intensity by a series of spherical harmonics. An approximate form of the equation of radiative transfer can then be obtained by truncating the series after a certain number of terms. It is known from neutron transport theory that the first approximation (called the P_1 approximation) is sufficiently accurate for most problems [9].

This paper illustrates reduction of the set of three radiation transport equations based on the spherical harmonic approximation to a two-flux form which makes approximate allowance for the two-dimensional radiative transfer for an idealised radiant cell of a multipass process gas heater. The basis of the reduction is to assume simple polynomial variation of some radiative quantities with radial position, and apply a radial averaging procedure. The new model is applicable to any axi-symmetrical system in which uniformity of velocity and concentration in every cross section normal to the axis of symmetry may reasonably be assumed. In addition, the calculations involved in its application are simple and economical enough to prove appealing to the industrial design engineer.

2. THE P_1 SPHERICAL HARMONIC EQUTIONS FOR AN AXI-SYMMETRICAL RADIATION FIELD

The idea of expressing the angular variation of radiative intensity at a point as a series of spherical harmonics has been developed and utilised extensively in the fields of astrophysics and neutron transport theory [9]. By using the P_1 approximation (in which the series is truncated after the first four terms) and the equation of radiative transfer, the axi-symmetrical radiation field within a grey non-scattering medium may be shown to be represented by the three following partial differential equations

$$\frac{1}{r}\frac{\partial}{\partial r}(rq_r)+\frac{\partial q_z}{\partial z}=K_a(4E_G-G) \tag{1}$$

$$\frac{\partial G}{\partial r}=-3K_a q_r \tag{2}$$

$$\frac{\partial G}{\partial z}=-3K_a q_z \tag{3}$$

where r and z are the radial and axial co-ordinates respectively, K_a is the volumetric absorption coefficient of the medium, E_G is its black body emissive power at the general point, G is the total incident flux density at the point, and q is the net radiant flux density in the positive co-ordinate direction denoted by the subscript.

The radiant flux densities in the positive and negative co-ordinate directions are simply related to G and q

$$q_\xi^+=\frac{G}{4}+\frac{q_\xi}{2}, \tag{4}$$

$$q_\xi^-=\frac{G}{4}-\frac{q_\xi}{2}, \quad \text{for } \xi=r, z \tag{5}$$

where q^+ and q^- are flux densities in the positive and negative co-ordinate directions denoted by the subscript.

3. REDUCTION OF THE RADIATION MODEL TO TWO-FLUX FORM

The general physical situation to be considered is that of a cylindrical enclosure containing a grey non-scattering medium in which combustion is taking place, and which is exchanging radiative energy with surrounding surfaces. In many industrial enclosures the curved bounding walls are composed of a mixture of refractory and sink surfaces. The most convenient method of treating the radiative exchange between the enclosed medium and such bounding surfaces is to imagine that the actual walls are replaced by an equivalent grey surface, whose emissivity and emissive power depend upon the emissivities and disposition of the various portions. Such an imaginary bounding grey surface will be assumed for the enclosure under consideration.

3.1 *Averaged form of the flux equations for the axial direction*

Multiplication of equations (1) and (3) by $r\,dr\,d\theta$ and integration over the circular cross section of the enclosure within the grey surface at height z gives

$$\frac{d\bar{q}_z}{dz} = K_a(4\bar{E}_G - \bar{G}) - \frac{2}{r_p}[(q_r)_{r=r_p}]_m \tag{6}$$

$$\frac{d\bar{G}}{dz} = -3K_a\bar{q}_z \tag{7}$$

where $[(q_r)_{r=r_p}]_m$ is the average net radial flux density to the grey surface defined by

$$[(q_r)_{r=r_p}]_m = \frac{1}{2\pi}\int_{\theta=0}^{\theta=2\pi}(q_r)_{r=r_p}\,d\theta \tag{8}$$

and where the bar over any quantity denotes its area weighted mean value over the cross section. For example,

$$\bar{q}_z = \frac{1}{\pi r_p^2}\int_{r=0}^{r=r_p}\int_{\theta=0}^{\theta=2\pi} q_z r\,dr\,d\theta \tag{9}$$

where θ is an angular co-ordinate (Fig. 1), and r_p is the radius of the grey cylindrical surface.

3.2 *Idealised model of the radiant cell of a process gas heater*

Equations (6) and (7) are applicable to any cylindrical enclosure. However, to illustrate the use of radial flux equation (2) for the evaluation of the flux density of radiation at the grey surface it is necessary to consider a particular enclosure. The example chosen is an idealised model of the radiant cell of a multipass process gas heater as shown in Fig. 1. Burners located at the bottom of the cell introduce the gas and air which burn and exchange radiative energy with the bounding refractory backed tubes carrying the process fluid, before exiting at the top. The tubes are arranged vertically along the sidewalls in N batches of n passes, the fluid being assumed to enter and leave each batch at the top of the cell in question, for which both N and n are even numbers. To simplify the theoretical treatment the tube arrangement is assumed to be as shown in Fig. 2, the figures on the tubes denoting the pass numbers.

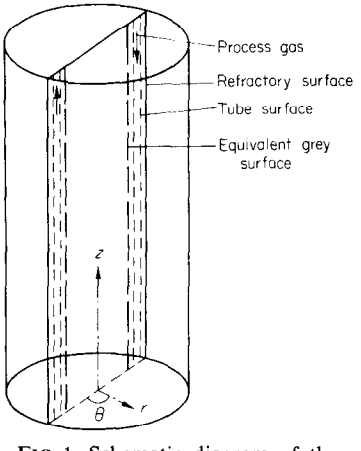

FIG. 1. Schematic diagram of the radiant cell of a typical process gas heater.

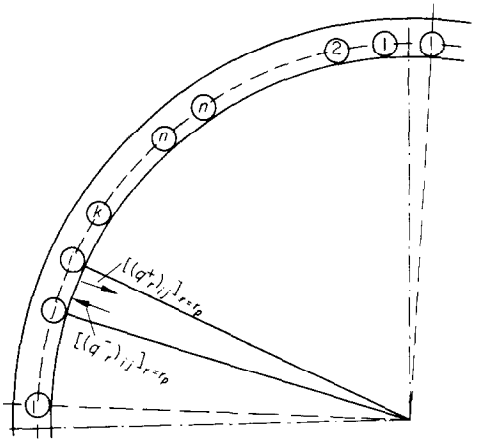

FIG. 2. Assumed tube arrangement.

Treatment of the radiative interchange between the furnace gas and the refractory backed tubes is based on the replacement of the tube-row backwall combination by a cylindrical grey surface tangential to the tubes on the furnace gas side. Details of the assumptions utilised in the imaginary grey surface treatment can be found elsewhere [10]. The expressions resulting from that treatment are introduced as required in the following sections.

3.3 *Determination of radiant flux densities at the grey surface for the radiant cell*

Equation (6) cannot be used for calculation purposes until the radiant flux densities at the grey surface have been expressed in terms of some other radiation parameters. This can be achieved by considering the variation of G in any cross section.

Due to the variation in tube surface temperature from tube to tube the flux densities of the radiation arriving at and leaving the grey surface will vary with angular position θ at any height. However, because of the assumed tube arrangement (Fig. 2), it is only necessary to consider a portion of the grey surface between $(2n+1)$ adjacent tubes, which includes $2n$ spaces between tubes, as the variation of the radiant flux density with θ will be repeated regularly for each group of $2n$ spaces. In Fig. 2 the flux density of radiation incident upon the grey surface between tubes i and j is denoted by $[(q_r^+)_{ij}]_{r=r_p}$, and the corresponding leaving flux density by $[(q_r^-)_{ij}]_{r=r_p}$. In practice both these quantities will vary continuously with θ over the space between the two tubes but to simplify subsequent theoretical treatment it is assumed that there is no variation of any quantity with θ in any small sector of the grey surface circle bounded by the radii from the furnace axis to the axes of a pair of adjacent tubes. Angular variation of the quantity under consideration is then allowed for approximately by a discontinuous change in the quantity in moving from any sector to an adjacent sector.

Values for the radiant flux densities at the grey surface can be found by considering the boundary conditions governing the variation of G in any cross section:

(a) For an even number of tube batches, each ij gap

will be diametrically opposite to another ij gap, and hence $(G)_{ij}$ will be distributed symmetrically about the furnace axis.

(b) The radiant boundary condition for the portion of the grey surface between the ith and jth tubes can be expressed in terms of the arriving and leaving flux densities as

$$[(q_r^-)_{ij}]_{r=r_p} = \varepsilon_p(E_p)_{ij} + (1-\varepsilon_p)[(q_r^+)_{ij}]_{r=r_p} \quad (10)$$

where ε_p is the effective emissivity of the equivalent grey surface, and $(E_p)_{ij}$ is the effective black body emissive power of the portion of the grey surface, which is related as follows to the emissive power of the tube surfaces

$$(E_p)_{ij} = \tfrac{1}{2}[(E_t)_i + (E_t)_j]. \quad (11)$$

If $(G)_{ij}$ is assumed to vary parabolically with r, and the parabola is made to satisfy the condition of axial symmetry and the condition at the grey surface, an expression results containing only one undetermined coefficient. The value of this coefficient can be found in terms of the average total flux density of incident radiation and the emissive power of tube surfaces by averaging the parabolic expression for $(G)_{ij}$ over the cross section. By utilising the completely specified parabolic form for $(G)_{ij}$, the net and incident radial radiant flux densities at the grey surface are finally determined from equations (2), and (2), (4) and (5) with $\xi = r$ respectively, and take the forms

$$[(q_r)_{r=r_p}]_m = \frac{Cr_p}{2}[\bar{G} - 4(E_t)_m] \quad (12)$$

$$[(q_r^+)_{ij}]_{r=r_p} = \frac{Cr_p}{2B\varepsilon_p}[B\bar{G} - 2(E_t)_m] + \left[1 - \frac{2Cr_p(B-\frac{1}{2})}{B\varepsilon_p}\right](E_p)_{ij} \quad (13)$$

where

$$(E_t)_m = \frac{1}{n}\sum_{i=1}^{n}(E_t)_i. \quad (14)$$

Constants B and C are related to the radiative properties and the cross sectional radius by the formulae

$$B = 1 + 4\frac{\left(\frac{2}{\varepsilon_p} - 1\right)}{3K_a r_p} \quad (15)$$

$$C = \frac{4}{3K_a r_p^2(B-\frac{1}{2})}. \quad (16)$$

3.4 *Radiant energy balances in two-flux form*

Averaging equations (4) and (5) with $\xi = z$ over the cross section and rearranging gives

$$\bar{q}_z = \bar{q}_z^+ - \bar{q}_z^- \quad (17)$$

$$\bar{G} = 2(\bar{q}_z^+ + \bar{q}_z^-). \quad (18)$$

Substituting from equations (12), (17) and (18) into equations (6) and (7) and solving simultaneously for the differential terms produces two ordinary differential equations in the averaged flux densities for the z direction

$$\frac{d\bar{q}_z^+}{dz} = 2K_a.\bar{E}_G + 2C(E_t)_m - (\tfrac{7}{4}K_a + C)\bar{q}_z^+ - (\tfrac{1}{4}K_a + C)\bar{q}_z^- \quad (19)$$

$$-\frac{d\bar{q}_z^-}{dz} = 2K_a.\bar{E}_G + 2C(E_t)_m - (\tfrac{7}{4}K_a + C)\bar{q}_z^- - (\tfrac{1}{4}K_a + C)\bar{q}_z^+. \quad (20)$$

These equations are the mathematical representation of the new two-flux model for the radiant cell, the two fluxes involved being $\bar{q}_z^+$ and $\bar{q}_z^-$. For other types of axi-symmetrical furnace the form taken by the equations will depend upon the relationship between the emissive powers of the equivalent grey surface and the sink surfaces.

4. ADDITIONAL EQUATIONS REQUIRED FOR PREDICTION OF THE THERMAL BEHAVIOUR OF A RADIANT CELL

To test the accuracy of the new two-flux radiation model it is necessary to carry out numerical calculations for a radiant cell with specified input and boundary conditions. Before this is possible, several additional equations are required. These are given below.

4.1 *Total energy balance on the furnace gas*

An additional equation containing $\bar{E}_G$ can be found by carrying out a total energy balance on the combustion products (furnace gas) in any cross section normal to the cylinder axis. To simplify the form taken by this equation it will be assumed that the velocity and chemical species concentrations are uniform over the cross section, that the effects of conductive and convective heat transfer are negligible, and that the specific heat of the furnace gas is independent of position and temperature. After utilising these assumptions the energy balance can be written as

$$\frac{d\bar{q}_G}{dz} = -\frac{d\bar{q}_z}{dz} - \frac{2}{r_p}[(q_r)_{r=r_p}]_m + \frac{\dot{m}_F}{A_G}\frac{df}{dz}Q \quad (21)$$

where $\bar{q}_G$ is the cross sectional average flux density of sensible energy in the furnace gas, $\dot{m}_F$ is the initial mass flow rate of fuel, A_G is the cross sectional area of the enclosure within the grey surface, Q is the net calorific value of the fuel, and f is the fraction of fuel burnt at height z. $\bar{q}_G$ can be related to the cross sectional average absolute temperature of the furnace gas $\bar{T}_G$ as

$$\bar{q}_G = \frac{\dot{m}_G}{A_G}c_G(\bar{T}_G - T_b) \quad (22)$$

where $\dot{m}_G$ is the mass flow rate of the furnace gas, c_G its mass specific heat and T_b some base temperature for measuring quantities of sensible heat. By utilising equations (6) and (18), equation (21) can be rewritten in the form required for calculation purposes

$$\frac{d\bar{q}_G}{dz} = 2K_a(\bar{q}_z^+ + \bar{q}_z^- - 2\bar{E}_G) + \frac{\dot{m}_F}{A_G}\frac{df}{dz}Q. \quad (23)$$

4.2 *Total energy balance for the process gas on its ith pass*

Assuming that within the process gas tubes heat is transferred from the inner wall to the fluid by convection alone, and that the specific heat of the process gas is independent of position and temperature, the total energy balance for the process gas on its ith pass

takes the form

$$(-1)^i \frac{\mathrm{d}}{\mathrm{d}z}[(q_g)_i] = \frac{\varepsilon_p}{nr_p}\{\langle[(q_r^+)_{ij}]_{r=r_p} + [(q_r^+)_{ik}]_{r=r_p} - 2(E_t)_i\rangle + \frac{S\beta r_p}{\varepsilon_p}[(E_t)_j + (E_t)_k - 2(E_t)_i]\}$$

where $(q_g)_i$ is the flux density of sensible energy in the process gas in the direction of flow on its ith pass (summed for all N ith passes) based on A_G, S is half the total tube surface area per unit volume of furnace gas space, and $(E_t)_i$ is the black body emissive power of the outer surface of the ith tube. ε_p and β are related to the emissivity of the tube surfaces (ε_t) and the radiation view factors by the expressions

$$\varepsilon_p = \frac{4F_{pt}(1-F_{pt})\varepsilon_t}{[1-(1-\varepsilon_t)(1-2F_{tp}+2F_{tp}F_{pt})]} \quad (25)$$

$$\beta = \frac{(1-2F_{tp}+F_{tp}F_{pt})\varepsilon_t^2}{[1+(1-\varepsilon_t)(1-2F_{tp})][1-(1-\varepsilon_t)(1-2F_{tp}+2F_{tp}F_{pt})]} \quad (26)$$

where F_{tp} is the view factor for half the surface of a tube to the grey surface, and F_{pt} is the view factor for the grey surface to half the surface of a tube.

$(q_g)_i$ is related to the absolute temperature of the process gas on its ith pass $[(T_g)_i]$ by the relationship

$$(q_g)_i = \frac{\dot{m}_g}{A_G} c_g[(T_g)_i - T_b] \quad (27)$$

where $\dot{m}_g$ is the total mass flow rate of the process gas and c_g its mass specific heat.

The working form of the total energy balance on the process gas is obtained by substituting from equation (13) into equation (24). After neglecting certain terms on the right hand side of the equation (Appendix A) the balance reduces to the simplified form

$$(-1)^i \frac{\mathrm{d}}{\mathrm{d}z}[(q_g)_i] = \frac{2C}{n}[\overline{q_z^+} + \overline{q_z^-} - 2(E_t)_i]. \quad (28)$$

4.3 *Energy balance on a tube wall*

The final equation necessary for numerical solution on the radiant cell is provided by an energy balance on the wall of the ith tube, which relates the process gas, furnace gas and outer tube surface temperatures.

$$\frac{(T_t)_i - (T_g)_i}{D} = \frac{C}{S}[\overline{q_z^+} + \overline{q_z^-} - 2(E_t)_i] \quad (29)$$

where

$$(E_t)_i = \sigma(T_t)_i^4 \quad (30)$$

and where σ is the Stefan–Boltzmann constant, and D is the overall thermal resistance between the outer surface of a tube and the process fluid based on unit area of the outer surface of the tube.

4.4 *Emissive power of the refractory surface*

The average emissive power of the sidewall refractory at any height $(E_R)_m$ is given by the relationship

$$(E_R)_m = \frac{[2F_{tp}(1-F_{pt}) + \varepsilon_t(1-2F_{pt}+2F_{tp}F_{pt})][(q_r^+)_{r=r_p}]_m + 2\varepsilon_t F_{pt}(E_t)_m}{[1-(1-\varepsilon_t)(1-2F_{tp}+2F_{tp}F_{pt})]}. \quad (31)$$

where the average incident flux density on the grey surface can be obtained from equation (13) as

$$[(q_r^+)_{r=r_p}]_m = \frac{Cr_p}{\varepsilon_p}(\overline{q_z^+} + \overline{q_z^-}) + \left(1 - \frac{2Cr_p}{\varepsilon_p}\right)(E_t)_m. \quad (32)$$

5. NUMERICAL SOLUTION FOR A PARTICULAR RADIANT CELL

In order to obtain detailed radiative heat flux and temperature distributions for a particular radiant cell it is necessary to solve simultaneous equations (19), (20), (22), (23) and (27)–(30) with $i = 1, 2, \ldots, n$. These equations involve the unknown variables $\overline{q_z^+}$, $\overline{q_z^-}$, $\overline{q_G}$, $\overline{T}_G$, $\overline{E}_G$, f and $(q_g)_i$, $(T_g)_i$, $(T_t)_i$, $(E_t)_i$ with $i = 1, 2, \ldots, n$, and before complete solution is possible the following additional information must be provided:

(i) A relationship between $\overline{T}_G$ and $\overline{E}_G$. For the idealised radiant cell considered the relationship is taken to be (Appendix B)

$$\overline{T}_G = (\overline{E}_G/\sigma)^{\frac{1}{4}}. \quad (33)$$

(ii) The cell and tube geometries and material properties, and initial conditions for the furnace gas, air, and process gas. The values used are based on an operating heater.

(iii) Radiative boundary conditions at the top and bottom of the radiant cell. The end walls are assumed to be radiatively adiabatic, with

$$\overline{q_z^+} = \overline{q_z^-} \quad \text{at} \quad z = 0 \quad \text{and} \quad z = L. \quad (34)$$

(iv) The combustion pattern. The pattern assumed is the simple polynomial form suggested by Roesler [11]

$$\left.\begin{aligned} f &= 3\left(\frac{z}{L_f}\right)^2 - 2\left(\frac{z}{L_f}\right)^3 \quad \text{for} \quad 0 \leqslant z \leqslant L_f \\ f &= 1 \quad \text{for} \quad L_f \leqslant z \leqslant L. \end{aligned}\right\} \quad (35)$$

where L_f is the flame length, defined as the distance from the burners at which combustion is complete.

The computational problem involves the solution of a number of simultaneous non-linear differential equations. The numerical solution procedure adopted is based on an iterative scheme coupled with combined two and three-point predictor–corrector methods for the numerical integration [12]. With 25 space increments in the vertical direction for numerical integration, convergence of the solution to the order of 10^{-5} W/m^2 in $\overline{q_z^-}$ at the heater inlet was obtained in about 30 iterative cycles, taking approximately 50 s of computing time on an ICL 1907 computer.

In order to provide numerical values of radiative heat flux and temperature as a basis of comparison for the values predicted using the two-flux model, all calculations have been repeated using the zone method of analysis for modelling the radiation field [13].

6. RESULTS OF CALCULATIONS AND DISCUSSION

The thermal behaviour of an idealised physical model of the radiant cell of a process gas heater has been predicted by the two-flux form of P_1 spherical harmonic approximation and the zone method of analysis, using the same input data for the computer programs of both methods. To demonstrate the effect of flame length on the predicted radiative behaviour of the heater, all calculations have been repeated with $L_f = 0$, and $L_f = 0{\cdot}48$L, the former corresponding to complete combustion at the burners, and the latter to the flame length observed in the heater under normal operating conditions.

For generality, all quantities are presented in dimensionless form, temperatures being made dimensionless by dividing them by the adiabatic flame temperature of the furnace gas (neglecting any dissociation) (T_{ad}), and radiative flux densities being made dimensionless by dividing them by the black body emissive power of the furnace gas at its adiabatic flame temperature (E_{ad}).

6.1 *Comparison of furnace gas temperature distributions*

Figures 3 and 4 illustrate the comparison of predicted furnace gas temperature distributions for $L_f = 0$ and $L_f = 0{\cdot}48$L respectively. It can be seen that the distributions follow the physically correct trends for both flame lengths, and that the furnace gas temperatures evaluated by the spherical harmonic approximation are in excellent agreement with those obtained by the zone method of analysis.

Comparison of Figs. 3 and 4 shows that the magnitude of the differences between the temperatures predicted using the two radiation models appear to be virtually independent of the heat release pattern.

The predicted furnace gas exit temperature for $L_f = 0{\cdot}48$L is 0·609 for both the two-flux and the zone methods, which differs by approximately 0·3 per cent from the value measured on the operating heater (0·611).

6.2 *Comparison of predicted net radiant flux density distributions*

Distributions of dimensionless arithmetic average net radiant flux densities to the surfaces of the tubes at any height for $L_f = 0$ and $L_f = 0{\cdot}48$L are shown in Figs. 5 and 6 respectively. Although the distributions follow common trends for both flame lengths, it can be seen there are distinct differences between the distributions predicted by the new method and the zone method, the flux densities being underpredicted in the regions of high furnace gas temperature, and overpredicted in the regions of low temperature. This can be attributed to the different bases of formulation of the flux density of radiation incident on the grey surface, which depends upon the flux densities of axial radiation in the immediately adjacent furnace gas at any height for the spherical harmonics method, and upon the radiation arriving from all other zones for the zone method of analysis.

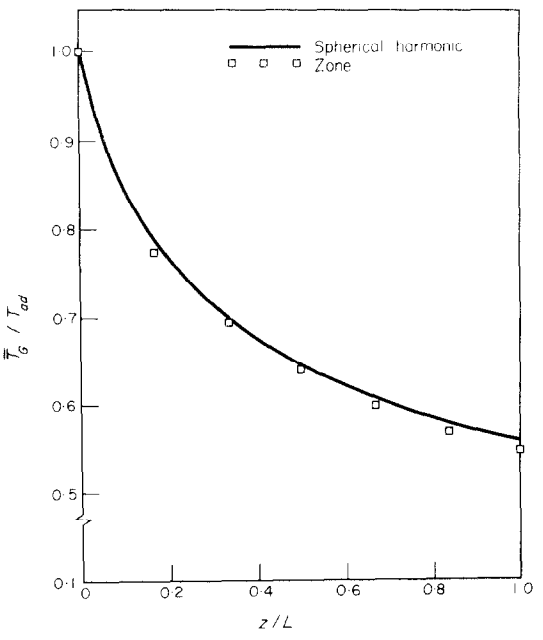

FIG. 3. Comparison of dimensionless furnace gas temperature distributions for $L_f = 0$.

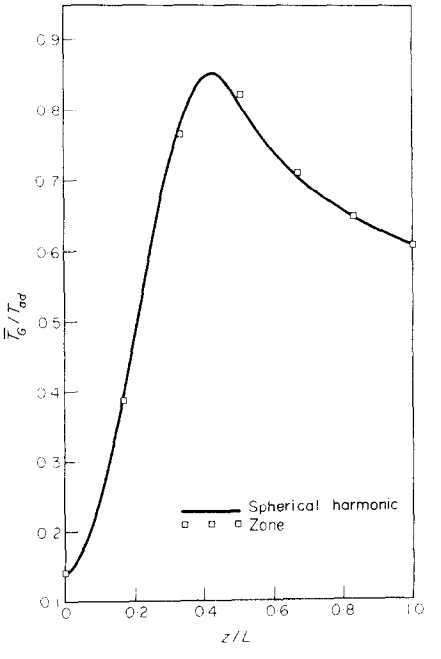

FIG. 4. Comparison of dimensionless furnace gas temperature distributions for $L_f = 0{\cdot}48L$.

6.3 *Comparison of tube surface temperature distributions*

Figure 7 compares the predicted distributions of the outer surface temperature of a tube containing the process fluid on its sixth and final pass for $L_f = 0{\cdot}48$L. This is the pass for which maximum temperatures occur and for which, therefore, tube material failure due to local overheating is most likely. The predicted distributions and the peak tube surface temperatures can be seen to be in close agreement. Comparison of Figs. 6 and 7 shows that the maximum tube surface temperature takes place at approximately the same

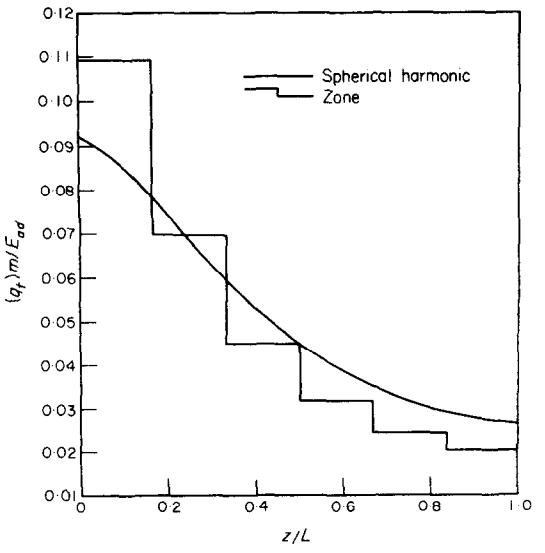

FIG. 5. Comparison of dimensionless average net flux densities to the tube surfaces for $L_f = 0$.

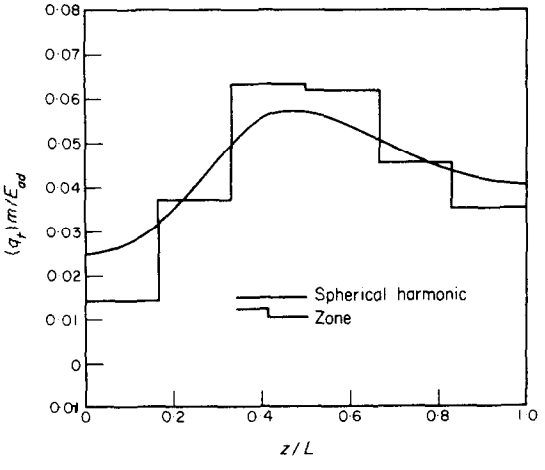

FIG. 6. Comparison of dimensionless average net flux densities to the tube surfaces for $L_f = 0{\cdot}48L$.

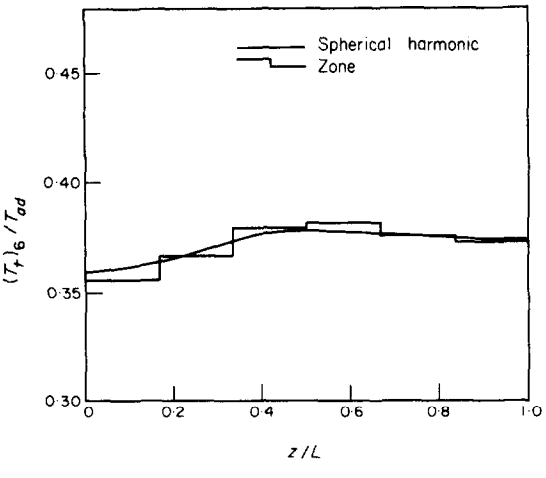

FIG. 7. Comparison of dimensionless tube surface temperatures for $i = 6$ and $L_f = 0{\cdot}48L$.

height as the maximum in the net flux density of radiation (as the two are closely related) for the spherical harmonic approximation but not for the zone method of analysis. This may be due to coarse zoning of the heater, which prevents the zone method from predicting the exact location and the magnitude of the maximum temperature.

6.4 *Comparison of process gas temperatures*

As a consequence of the high ratio of the product of mass flow rate and specific heat for the process gas to that for the furnace gas ($\dot{m}_g c_g/\dot{m}_G c_G = 7{\cdot}46$) for the heater considered, the variation of the process gas temperature along the heater in any pass is relatively small. Therefore, instead of attempting to present distributions in graphical form, a few typical values of interest will be given. The exit process gas temperature is

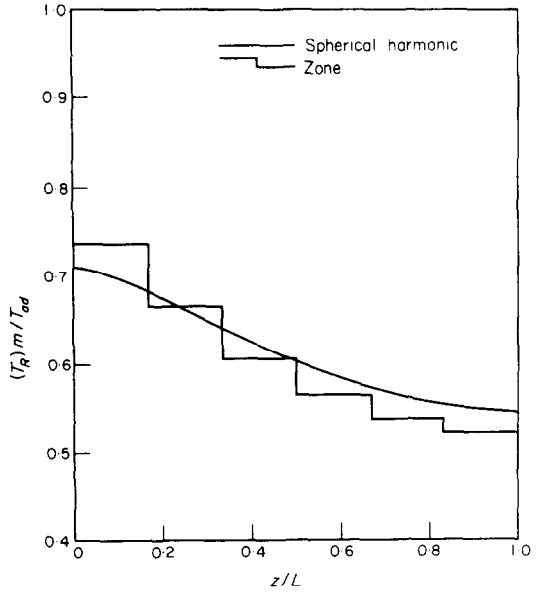

FIG. 8. Comparison of dimensionless sidewall refractory temperatures for $L_f = 0$.

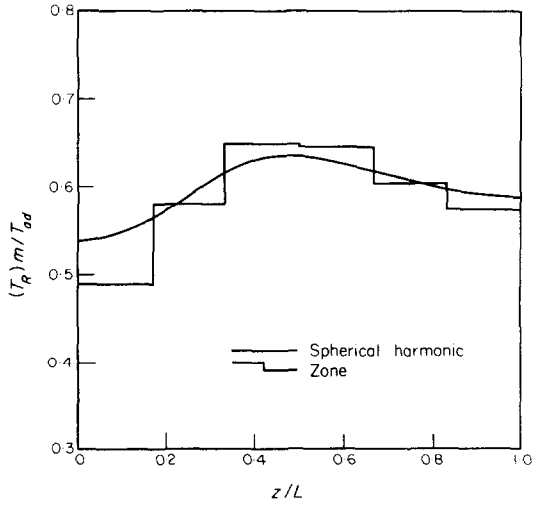

FIG. 9. Comparison of dimensionless sidewall refractory temperatures for $L_f = 0{\cdot}48L$.

predicted to be 0·359 for both the spherical harmonics and the zone methods, which is identical with the value of 0·359 which was measured on the heater.

It is also found that the predicted arithmetic average process gas temperature, taken over all six passes at any height, varies negligibly with position over the whole height of the heater, being 0·333 for the spherical harmonics method, as compared with 0·332 for the zone method. This means that, on average, the furnace gas is losing heat to a sink at essentially constant temperature during its passage through the heater.

6.5 *Comparison of temperature distributions for refractory*

Average sidewall refractory temperature distributions for $L_f = 0$ and $L_f = 0{\cdot}48L$ are illustrated in Figs. 8 and 9 respectively. It can be seen that the refractory temperature distributions display the same patterns as the net flux density distributions for both flame lengths (Figs. 5 and 6). This is to be expected, as the emissive power of the radiatively adiabatic refractory wall depends upon the flux density of incident radiation, which in turn determines the net flux to the refractory backed tubes.

7. CONCLUSIONS

A new two-flux treatment of the two-dimensional radiative transfer in axi-symmetrical enclosures has been derived from equations based on the P_1 spherical harmonic approximation, and applied to the investigation of the thermal behaviour of an idealised model of the radiant cell of a multipass process gas heater. Comparison of the results of the treatment with zone method calculations and some experimentally determined values has demonstrated that its predictions of temperature distributions and overall thermal performance are of acceptable accuracy. As a result of this predictive accuracy, coupled with its computational simplicity and economy relative to the zone method of analysis, the two-flux model should prove useful to design engineers for prediction of the thermal behaviour of axi-symmetrical furnaces and combustors in which cross-sectional uniformity of velocity and species concentrations may reasonably be assumed.

REFERENCES

1. W. E. Lobo and J. E. Evans, Heat transfer in the radiant section of petroleum heaters, *Trans. Am. Inst. Chem. Engrs* **35**, 743 (1940).
2. H. C. Hottel, Radiative transfer in combustion chambers, *J. Inst. Fuel* **34**, 220 (1961).
3. H. C. Hottel, First estimates of industrial furnace performance—the one-gas-zone model re-examined, in *Heat Transfer in Flames* (edited by N. H. Afgan and J. M. Beér), p. 5. Scripta, Washington D.C. (1974).
4. A. D. Gosman and F. C. Lockwood, Incorporation of a flux model for radiation into a finite difference procedure for furnace calculations, 14th Symposium (Intern.) on Combustion, The Combustion Inst., Pittsburgh, Pa, 661 (1973).
5. S. V. Patankar and D. B. Spalding, Simultaneous predictions of flow pattern and radiation for three-dimensional flames, in *Heat Transfer in Flames* (edited by N. H. Afgan and J. M. Beér), p. 73. Scripta, Washington DC (1974).
6. H. C. Hottel and A. F. Sarofim, *Radiative Transfer*. McGraw-Hill, New York (1967).
7. T. M. Lowes, H. Bartelds, M. P. Heap, S. Michelfelder and B. R. Pai, Prediction of radiant heat flux distribution. I.F.R.F., Doc. No. G 02/a/26 (1973).
8. W. Richter and R. Quack, A mathematical model of a low-volatile pulverised fuel flame, in *Heat Transfer in Flames* (edited by N. H. Afgan and J. M. Beér), p. 95. Scripta, Washington DC (1974).
9. B. Davison, *Neutron Transport Theory*. Oxford University Press, London (1958).
10. N. Selçuk, R. G. Siddall and J. M. Beér, Prediction of the effect of flame length on temperature and radiative heat flux distributions in a process fluid heater, *J. Inst. Fuel* **48**, 89 (1975).
11. F. C. Roesler, Theory of radiative heat transfer in co-current tube furnaces, *Chem. Engng Sci.* **22**, 1325 (1967).
12. R. G. Siddall and N. Selçuk, The application of flux methods to prediction of the behaviour of a process gas heater, in *Heat Transfer in Flames* (edited by N. H. Afgan and J. M. Beér), p. 191. Scripta, Washington DC (1974).
13. N. Selçuk, R. G. Siddall and J. M. Beér, A comparison of mathematical models of the radiative behaviour of an industrial heater, *Chem. Engng Sci.* **30**, 871 (1975).

APPENDIX A

Omission of Terms in Process Gas Energy Balance

Substitution from equations (11) and (13) into equation (24) leads to the following balance equation for the process gas on its ith pass

$$(-1)^i \frac{\mathrm{d}}{\mathrm{d}z}[(q_g)_i] = \frac{2C}{n}[\overline{q_z^+} + \overline{q_z^-} - 2(E_t)_i](1+\phi) \quad \text{(A.1)}$$

where

$$\phi = \frac{\left(\frac{1}{2B} - 1 + \frac{\varepsilon_p}{2Cr_p} + \frac{S\beta}{C}\right)[(E_t)_j + (E_t)_k - 2(E_t)_i] - \frac{2}{B}(E_t)_m}{[\overline{q_z^+} + \overline{q_z^-} - 2(E_t)_i]}. \quad \text{(A.2)}$$

In the working equations used in the calculations ϕ is neglected compared with 1. At the conclusion of calculations, the predicted temperatures were used to estimate the value of ϕ. Its maximum order of magnitude was found to be $-0{\cdot}01$, and it was therefore concluded that neglect of ϕ would not lead to any substantial errors in the predicted temperatures and heat fluxes.

APPENDIX B

Replacement of $\bar{T}_G$ by $(\bar{E}_G/\sigma)^{\frac{1}{4}}$

The average furnace gas temperature at any height may be defined by the relationship

$$\bar{T}_G = \frac{1}{\pi r_p^2}\int_{r=0}^{r=r_p}\int_{\theta=0}^{\theta=2\pi} T_G r\,\mathrm{d}r\,\mathrm{d}\theta = \frac{2}{r_p^2}\int_{r=0}^{r=r_p}(T_G)_m r\,\mathrm{d}r. \quad \text{(B.1)}$$

If peripheral variation of furnace gas temperature around any circle of radius r is now neglected, $(T_G)_m$ may be expressed in terms of $(E_G)_m$ as

$$(T_G)_m = [(E_G)_m/\sigma]^{\frac{1}{4}}. \quad \text{(B.2)}$$

For the two-flux form of P_1 spherical harmonic approximation $(E_G)_m$ takes the following form

$$(E_G)_m = \psi - 2(\psi - \bar{E}_G)\frac{r^2}{r_p^2} \quad \text{(B.3)}$$

where

$$\psi = \frac{B}{(B-\frac{1}{2})}\bar{E}_G - \frac{C}{8K_a(B-\frac{1}{2})}\bar{G} - \frac{(K_a - C)}{2K_a(B-\frac{1}{2})}(E_t)_m + \frac{1}{6K_a^2(B-\frac{1}{2})}\frac{\mathrm{d}^2(E_t)_m}{\mathrm{d}z^2}.$$

Substituting from equations (B.2) and (B.3) into equation (B.1) and performing the integration, followed by binomial expansion gives

$$\bar{T}_G = \left(\frac{\bar{E}_G}{\sigma}\right)^{\frac{1}{4}}\left[1 - \tfrac{1}{32}\left(\frac{\psi}{\bar{E}_G} - 1\right)^2 + \ldots\right]. \qquad \text{(B.4)}$$

The assumption in the calculations that $\bar{T}_G$ is equal to $(\bar{E}_G/\sigma)^{\frac{1}{4}}$ is therefore justifiable if $\frac{1}{32}[(\psi/\bar{E}_G) - 1]^2$ and the subsequent terms in the expansion small compared with unity. Use of the predicted temperatures showed that the maximum order of magnitude of $\frac{1}{32}[(\psi/\bar{E}_G) - 1]^2$ occurred at the heater entrance and was less than 10^{-3}, and it was therefore concluded that its neglect would lead to insignificant errors.

MODELISATION A DEUX FLUX DU TRANSFERT BIDIMENSIONNEL PAR RAYONNEMENT DANS LES FOURS A L'AIDE DES HARMONIQUES SPHERIQUES

Résumé—Un nouveau modèle à deux flux pour les champs de rayonnement bidimensionnels dans les fours axisymétriques a été obtenu à partir des équations de transfert du rayonnement, basées sur l'approximation P_1 des harmoniques sphériques, en supposant une variation radiale polynomiale de quelques paramètres de rayonnement et en effectuant une moyenne. Le nouveau modèle a été appliqué à la prévision du comportement thermique d'une cellule de rayonnement idéale de réchauffeur de gaz à plusieurs passages. Les résultats ont été comparés avec les valeurs obtenues antérieurement soit par la méthode des zones, soit par des mesures limitées sur un réchauffeur en fonctionnement. On a obtenu des prévisions satisfaisantes pour les distributions de température dans le gaz et sur la paroi, ainsi que pour le comportement thermique global de la cellule. Cet accord, joint à la simplicité et à l'économie des calculs par rapport à la méthode des zones, suggère que les modèles à deux flux de ce type devraient s'avérer utiles pour approcher les calculs thermiques dans les projets de fours et de foyers axisymétriques.

EIN ZWEIFLUSS-KUGEL-HARMONISCHES MODELL DES ZWEIDIMENSIONALEN STRAHLUNGSAUSTAUSCHES IN ÖFEN

Zusammenfassung—Ein neues Zweiflussmodell für zweidimensionale Strahlungsfelder in axsymmetrischen Öfen wurde hergeleitet aus Gleichungen des Strahlungstransportes die auf der P_1 kugelharmonischen Näherung beruhen. Dazu wurde eine Radial-Polynom-Variation einiger Strahlungsparameter angenommen und ein Mittelungsverfahren angewandt. Das neue Modell wurde angewandt zur Bestimmung des thermischen Verhaltens einer idealisierten strahlenden Zelle eines Multipass-Prozessgasheizers. Die Ergebnisse wurden mit früher erhaltenen Werten verglichen, die auf der Zonenanalysis-Methode beruhen und mit einer geringen Zahl experimenteller Werte aus einem betriebenen Heizer. Zufriedenstellende Aussagen ergaben sich für die Gasoberflächen-Temperaturverteilungen und für das thermische Gesamtverhalten der Zelle. Die Voraussagegenauigkeit zusammen mit der rechnerischen Einfachheit im Vergleich zur Zonenanalysis-Methode zeigt, dass das hier benützte Zweiflussmodell für thermische Auslegungsberechnungen von axsymmetrischen Öfen und Brennern nützlich ist.

МОДЕЛИРОВАНИЕ ДВУМЕРНОГО ЛУЧИСТОГО ПЕРЕНОСА В ПЕЧАХ С ПОМОЩЬЮ СФЕРИЧЕСКИХ ГАРМОНИК

Аннотация — На основании аппроксимации сферическими гармониками P_1 с учетом радиального полиномиального изменения некоторых параметров излучения и с помощью усреднения из уравнений лучистого переноса выведена двухпотоковая модель для двумерных полей излучения в осесимметричных печах. Новая модель использовалась для расчета теплового режима идеализированной излучающей ячейки газового многоходового нагревателя. Результаты расчета сравнивались со значениями, полученными ранее с помощью зонального метода анализа, а также проверялись на ограниченном числе экспериментальных данных, измеренных во время работы нагревателя. Получены удовлетворительные результаты по распределению температуры газа и поверхности и по суммарному тепловому режиму ячейки. Точность расчета вместе с его простотой и экономичностью в сравнении с зональным методом анализа свидетельствуют в пользу моделей этого типа при расчетах осесимметричных печей и камер сгорания.